

Electric field lines near an oddly shaped conductor in a uniform electric field

Ross L. Spencer

Citation: *American Journal of Physics* **56**, 510 (1988); doi: 10.1119/1.15567

View online: <http://dx.doi.org/10.1119/1.15567>

View Table of Contents: <http://scitation.aip.org/content/aapt/journal/ajp/56/6?ver=pdfcov>

Published by the [American Association of Physics Teachers](#)



Re-register for Table of Content Alerts

Create a profile.



Sign up today!



Electric field lines near an oddly shaped conductor in a uniform electric field

Ross L. Spencer

Department of Physics, Brigham Young University, Provo, Utah 84602

(Received 18 June 1987; accepted for publication 18 September 1987)

Physics textbooks almost always contain at least one picture of an oddly shaped conductor, usually in the section discussing Gauss' law and the charged conductor. It is, however, rare to see a representation of the field lines in the neighborhood of such a conductor. This article discusses the problem of an arbitrarily shaped uncharged conductor imbedded in an otherwise uniform electric field. The method of successive overrelaxation is used to compute the electrostatic potential from which the electric field lines are computed by numerical integration.

One of the intriguing topics in the study of electrostatics is the property that any excess charge on a conductor resides on its surface. In most textbooks where this property is discussed a picture of an oddly shaped conductor appears. Less common is a representation of the field lines in the neighborhood of such an object. The reason for this omission is quite simple: Electric fields are difficult to compute in the presence of asymmetric equipotential surfaces. A nice aid to the developing intuition of physics students would be a few accurately drawn field lines in the presence of such a conductor. If possible, the lines should illustrate the property that the density of lines is proportional to the magnitude of the electric field. (Note that this is not easy to achieve; in a fully asymmetric geometry, there may not be any suitable set of field lines that could be represented on the flat page. Furthermore, if the equipotential surfaces are not infinitely long and uniform in at least one of the three Cartesian dimensions, then the density of lines on a flat surface is not the same as the density of lines in three-dimensional space.) This article describes a method of computing such a set of field lines for oddly shaped conductors.

As an illustration of the method, the case of an uncharged conductor in an otherwise uniform electric field is discussed. To make sure that a set of field lines lying in a plane exists, the intersection of the surface of the conductor with the xy plane is assumed to be given by the function

$$r = g(\theta), \quad (1)$$

where $r = (x^2 + y^2)^{1/2}$ and where $\tan \theta = y/x$. Figure 1 shows the intersection with the xy plane of the oddly shaped conductor used in these calculations. It was obtained by drawing the shape freehand on a sheet of graph paper, choosing an interior point as the origin of plane polar coordinates, dividing the angular interval $[0, 2\pi]$ into 32 subintervals, and measuring the radius to the surface at the edge of each subinterval. Lagrange three-point interpolation¹ was then used to obtain $g(\theta)$ at arbitrary angles θ . The conductor surface is assumed to extend symmetrically above and below the xy plane so that a field line started in the xy plane remains in this plane. At each value of z above and below the xy plane, the shape at $z = 0$ is replicated and reduced, becoming ever smaller in size until it finally shrinks to zero at $z = \pm z_c$. This sounds complicated, but its mathematical realization is quite simple:

$$\frac{z^2}{z_c^2} + \frac{x^2 + y^2}{g^2(\theta)} = 1. \quad (2)$$

By adjusting the value of z_c , various shapes may be studied. In this article, two cases will be discussed. (1) The "spherical" case denotes the use of a value of z_c that is equal to the average radius of the conductor surface in the xy plane. Figure 2 illustrates the appearance of the surface of the conductor for this case. (2) The "cylindrical" case denotes the use of a value of z_c that is very much larger than the average radius of the conductor surface. This means that near the xy plane the electrostatic potential ϕ is uniform in z , so the problem is only two dimensional in this case.

With the conductor thus specified, the electrostatic problem may be stated: Find the electrostatic potential corresponding to a uniform electric field, $\mathbf{E} = E_0 \hat{x}$, for points

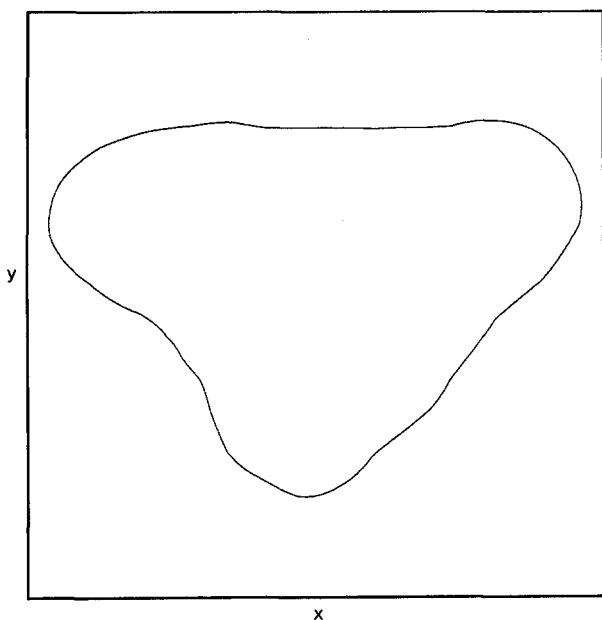


Fig. 1. The intersection with the xy plane of the oddly shaped conductor.

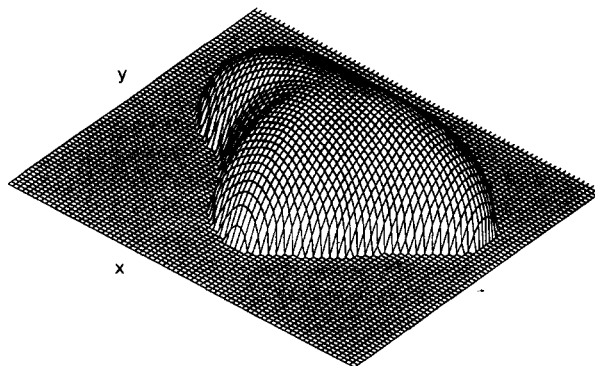


Fig. 2. A three-dimensional view in the spherical case of the oddly shaped conductor.

far from the conductor and having constant value ϕ_c on the surface of the conductor. Furthermore, adjust the value of ϕ_c so that the conductor has no net charge. The problem is solved by using the method of successive overrelaxation^{2,3} on a rectangular three-dimensional grid, in the spherical case, or on a two-dimensional grid, in the cylindrical case. The computing region is bounded by the six planes $x = \pm x_b$, $y = \pm y_b$, and $z = \pm z_b$, and the grid spacings in each direction are Δx , Δy , and Δz . To solve the problem, boundary conditions must be specified on the bounding plane surfaces and on the conductor. If x_b , y_b , and z_b were taken to be much larger than the dimensions of the conductor, it would be sufficient to let the potential on the outer surface be given by $\phi = -E_0 x$. This would be very inefficient, however, since only a few of the grid points would be in the neighborhood of the conductor where the solution is interesting. It is better to take for the potential on the outer boundary

$$\phi = -E_0 x \{1 - a^3 / [(x^2 + y^2 + z^2)^{3/2}]\}, \quad (3)$$

in the spherical case, and

$$\phi = -E_0 x [1 - a^2 / (x^2 + y^2)], \quad (4)$$

in the cylindrical case. The variable a is the average radius

$$\langle \phi^{n+1} \rangle = \frac{(1/\Delta x^2)(\phi_{x-}^n + \phi_{x+}^n) + (1/\Delta y^2)(\phi_{y-}^n + \phi_{y+}^n) + (1/\Delta z^2)(\phi_{z-}^n + \phi_{z+}^n)}{2(1/\Delta x^2 + 1/\Delta y^2 + 1/\Delta z^2)}, \quad (5)$$

where $\phi_{x-}^n = \phi^n(x - \Delta x, y, z)$, $\phi_{x+}^n = \phi^n(x + \Delta x, y, z)$, and, similarly, for y and z . The superscript on ϕ denotes the iteration level. Repeatedly computing this quantity for nonboundary points and replacing the value of ϕ at these points by the average above gives the relaxation algorithm. Convergence may be accelerated, however, by overrelaxing as follows:

$$\phi^{n+1} = \alpha \langle \phi^{n+1} \rangle + (1 - \alpha) \phi^n, \quad (6)$$

where α is a number between 1 and 2. By properly choosing α , the convergence may be substantially accelerated over simple relaxation ($\alpha = 1$). For oddly shaped regions like this one, there is no theory to help in determining the optimum value of α . In practice, a value around 1.5 seems to work pretty well. Convergence was also accelerated by using updated values on the right-hand side of Eq. (5) when they were available. This is easily implemented by simply having a single array of values of ϕ . This procedure is repeated until successive iterates of ϕ do not change by very much. Care must be taken in choosing a stopping point or the solution may be inaccurate.⁴ In the computations performed here, iteration continued until the rate of convergence was no longer greater than zero, i.e., until roundoff prevented further refinement of the solution. To help assure the physical significance of the solutions, the case of a circular cylindrical conductor was computed using this method and compared with the analytic result. The field lines in the two cases agreed to within the distance between grid points near the conductor and agreed more nearly away from the conductor. Tests were also made to determine the smallest possible values of x_b , y_b , and z_b so that high resolution in the neighborhood of the conductor could be obtained. It was found that for the conductor used here, having an average radius in the xy plane of 0.64, $x_b = y_b = z_b = 2.0$ was adequate.

of the conductor, and these formulas are simply the solutions to the electrostatic problem at hand for the case where the conductor shape in the xy plane is a circle of radius a . Using this form for the boundary conditions allows x_b , y_b , and z_b to be only a few times larger than the conductor radius a without losing accuracy. Specifying the potential on the conductor is more difficult because it does not fit the rectangular coordinate system. Fortunately, computers are now large enough and fast enough to make it possible to simply approximate the conductor shape by a sequence of steps without losing too much accuracy. Hence, if a grid point is inside the conductor surface, it is assigned the potential value ϕ_c . This leads to some roughness near the surface of the conductor but, by choosing a fine enough grid, this roughness is not noticeable. (In practice, this roughness means that field lines near the conducting surface may be in error by the distance between grid points.)

With the boundary conditions specified, the potentials at all other grid points must now be determined. This is accomplished by means of the successive overrelaxation algorithm. The first step is to compute for all grid points not on the outer boundary or inside the conductor the following weighted average:

Once the potential has been computed, the electric field must be computed so that the electric field line equations can be integrated. These equations are

$$\frac{dx}{ds} = \frac{E_x}{E}, \quad \frac{dy}{ds} = \frac{E_y}{E}, \quad (7)$$

where s is arclength along the line and where $E = (E_x^2 + E_y^2)^{1/2}$. The electric field was obtained by taking the gradient of the six-point bivariate interpolation formula for the potential.¹ This allows the electric field to be computed at arbitrary values of x and y . The field line equations were then integrated using the second-order Runge-Kutta algorithm.¹ It was desired to produce a picture corresponding to the case of an uncharged conductor. Because of the somewhat spherical shape of the conductor and its location near the center of coordinates, it is approximately correct to assign the conductor a potential of zero. However, when the field lines were integrated with $\phi_c = 0$, it was clear that field lines were originating on the conductor, indicating that it was positively charged. To eliminate this problem, Gauss' law was used in the xy plane to compute the total charge, and a new conductor potential was chosen to reduce the charge. This was done successively until the charge was sufficiently small that it had no noticeable effect on the field line pictures.

The results of these calculations in the spherical and cylindrical cases are shown in Figs. 3 and 4. In both figures, there are 100 grid points in each direction. Note that for the spherical case this required applying the successive overrelaxation algorithm to a $100 \times 100 \times 100$ array. The computation in this case took 4 h of CPU time on a VAX 8600. The field lines were started at the left edge of the frame, and care was taken to make sure that the spaces between neighboring lines at the left edge contained equal amounts of

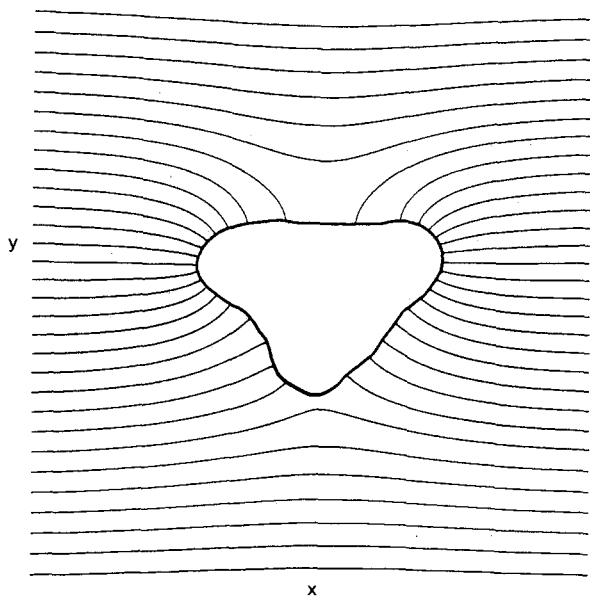


Fig. 3. The field lines in the xy plane in the neighborhood of the conductor shown in Fig. 2 (spherical case).

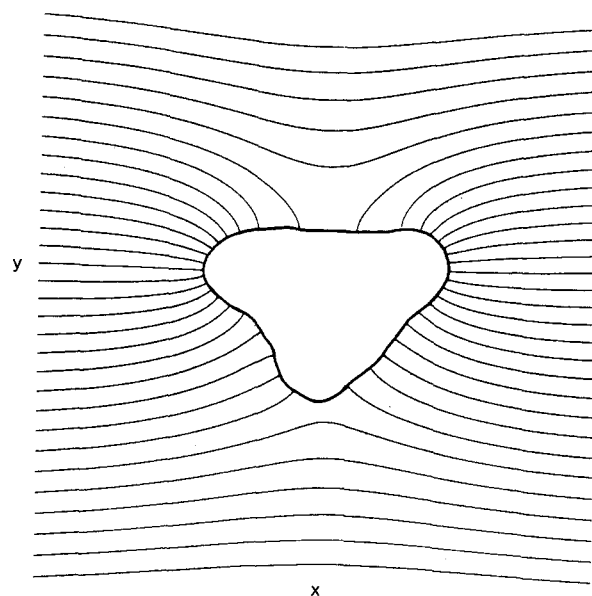


Fig. 4. The field lines in the xy plane in the neighborhood of the conductor in the cylindrical case, i.e., in the case that the conductor is highly elongated in the z direction.

electric flux, ensuring that the field line density is proportional to the electric field. The lines that terminate on the conductor must somehow be continued outward from the conductor to the right edge. This was accomplished by integrating backwards from the right edge, making sure that the electric flux at the starting point on the right edge was the same as that of the corresponding line at the left edge. After the lines were computed, they were drawn with an Imagen laser printer.

Figures 3 and 4 illustrate common features of electrostatic fields. The field lines are spaced relatively far apart at the top and at the bottom of the conductor. This is the case because the left and right sides of the conductor have opposite signs, so the surface charge density and the surface electric field must vanish along a line on the conductor surface separating the left and right sides. This line evidently passes near the center of the top and near the center of the bottom. The field lines are also relatively closely spaced on the bumps near the top on both the left and right sides. This behavior is commonly explained by saying that the curvature is large in these locations, so the surface field must also be large. Care must be taken in using this simple explanation, however, because it is generally untrue.⁵ In comparing the spherical and cylindrical cases, it is clear that in the spherical case the field becomes uniform more rapidly with increasing distance from the conductor than in the cylindrical case. This is simply because the spherical multipole potentials fall off more rapidly with distance from the source than do cylindrical multipole potentials.

It is thus not too difficult to solve complex electrostatic problems and, from the solution, to construct correctly drawn field lines by using standard numerical techniques on modern computers. Some textbooks contain poorly drawn figures illustrating electric field lines⁶ and many textbooks probably contain old figures that were drawn before accurate calculations coupled with high-quality graphics were possible. This is perhaps a good time for writers of textbooks to reconsider their figures and to produce for the next generation of students accurately drawn illustrations of electric field lines.

ACKNOWLEDGMENTS

The author acknowledges useful discussions with Dr. John Merrill. The plots were made with the Plasma Physics Plotting Package produced by groups CTR-10 and CTR-6 at the Los Alamos National Laboratory. The author gratefully acknowledges the assistance of Lise Chrien of CTR-10 for making this package available.

¹M. Abramowitz and I. A. Stegun, *Handbook of Mathematical Functions* (U. S. Government Printing Office, Washington, DC, 1964), Chap. 25.

²D. A. Hastings, *Am. J. Phys.* **43**, 518 (1975).

³M. DiStasio and W. C. McHarris, *Am. J. Phys.* **47**, 440 (1979).

⁴B. Kaplan, *Am. J. Phys.* **50**, 967 (1982).

⁵R. H. Price and R. J. Crowley, *Am. J. Phys.* **53**, 843 (1985).

⁶L. Kristjansson, *Phys. Teacher* **23**, 202 (1985).